Pressure Effects of Neon and Argon on the 535 nm Thallium Line*

R. S. Dygdała, R. Bobkowski, E. Lisicki, and J. Szudy
Institute of Physics, Nicholas Copernicus University, Grudzidzka 5/7, 87-100 Toruń, Poland

Z. Naturforsch. **42 a**, 559–564 (1987); received February 2, 1987

Experimental studies of collisional broadening and shift of the 535 nm thallium line perturbed by neon and argon were performed using a pressure-scanned Fabry-Perot interferometer. The 535 nm line was excited by irradiation of the thallium vapour with the resonance thallium line (377.68 nm). The present results are compared with previous experimental data obtained by different methods as well as with theoretical ones.

1. Introduction

This paper describes experimental studies of the collisional broadening and shift of the 535 nm line of thallium perturbed by neon and argon. The pressure effects of noble gases on this line were studied by Cheron et al. [1] who performed line shape measurements on the fluorescence light emitted from a mixture of natural thallium vapour and noble gas at rather high density ($(6.5-19.5) \times 10^{18}$ cm^{-3}). They determined the width and shift parameters corresponding to the Lorentzian profile of this line. The Lorentzian distribution is a typical feature of the impact theory of pressure broadening and it is usually valid at low densities. However, in the density range used in the experiments described in [1] the applicability of the impact theory becomes questionable. For this reason, we recently performed in this laboratory a series [2,3] of experiments on the collisional broadening and shift of the 535 nm Tl line by foreign gases at much lower densities than those used by Cheron et al. [1]. In this density region the impact theory is fully applicable. On the other hand, however, in experiments described in [2, 3] the atomic fluorescence of thallium was excited by the photodissociation of thallium iodide (TlI) molecules. This technique of excitation may introduce a certain error to the Lorentzian width and shift parameters determined from the total line profile measured by means of a Fabry-Perot interferometer. This error is connected with the fact that the atomic fluorescence line emitted by a fragment atom excited due to the photodissociation of the parent molecule exhibits an additional Doppler broadening arising from the recoil of the excited atom after the dissociation. The resultant Doppler shape of the atomic fluorescence line may differ significantly from the Gaussian distribution corresponding to the usual thermal Doppler broadening [4] and this makes the accurate interpretation of the measured values of the line shape parameters very difficult.

For this reason it is desirable to have further measurements for low pressures performed under conditions allowing for a precise determination of pressure broadening and shift coefficients. In the present work, in order to avoid possible errors connected with the non-Gaussian distribution of the Doppler broadening as in our earlier experiments performed by means of the photodissociation technique, the 535 nm line was excited by the irradiation of the thallium vapour with the resonance thallium line (377.68 nm). High-resolution spectroscopy techniques were used to measure the profiles of the 535 nm fluorescence line emitted by thallium vapour mixed with a perturbing gas (neon and argon).

2. Experimental

The fluorescence 535 nm Tl line (see Fig. 1) was analysed by means of a grating spectrograph with a

* This work was carried on under the Research Program CPBP 01.06.

Reprint requests to Dr. R. S. Dygdała, Institute of Physics, Nicholas Copernicus University, Grudzidzka 5/7, 87-100 Toruń, Polen.

0932-0784 / 87 / 0600-0559 $ 01.30/0. – Please order a reprint rather than making your own copy.

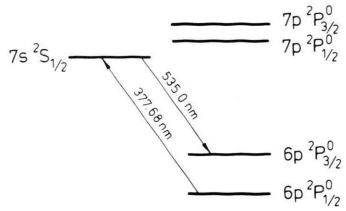

Fig. 1. Schematic diagram of the lowest energy levels of neutral thallium.

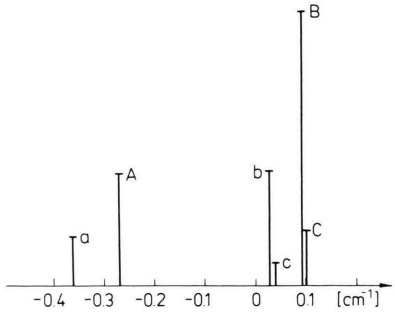

Fig. 2. Positions and relative intensities of the hyperfine structure components of the 535 nm Tl line. *A*, *B*, and *C* denote the hfs components for ^{205}Tl; *a*, *b*, and *c* denote those for ^{203}Tl.

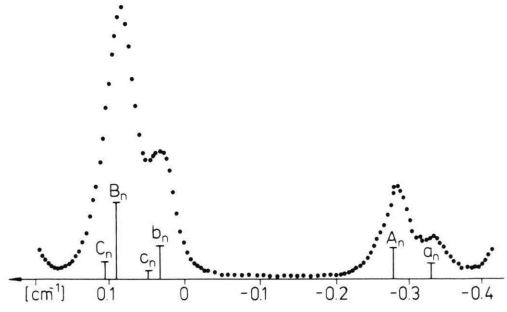

Fig. 3. Fabry-Perot interferogram of the 535 nm Tl line taken at the particle density $N = 0.9 \times 10^{17}$ cm^{-3} of Ne with the spacer of 0.845 cm.

Fabry-Perot interferometer using photoelectric detection [5]. The 535 nm line was emitted from a fluorescence cell 3.4 cm long and 2.8 cm in diameter. The intensity distribution was monitored using a photomultiplier in a photon counting mode. The pressure-scanned Fabry-Perot interferometer was used with plates coated with a dielectric layer, and spacers of 1.204 cm and 0.845 cm were applied. Two low pressure r.f. electrodeless thallium discharge lamps were used: one served as the reference source in the line shift measurements and the second one with a 377.68 nm filter was applied to excite the green fluorescence at 535 nm of thallium vapour in the cell. The fluorescence quartz cell with thallium vapour was mounted in an Al-block oven which was operated at a temperature of 793 K with a stability of $\pm$ 2 K over several hours. The temperature of the fluorescence cell was measured with a thermocouple which was placed in contact with this cell. All measurements were performed at a temperature of 793 K for various densities of neon and argon in the region between 9.5×10^{16} cm^{-3} and 7.0×10^{17} cm^{-3}.

3. Analysis of the Profiles

Natural thallium consists of two isotopes: 29.46% of ^{203}Tl and 70.54% of ^{205}Tl. The wave numbers and relative intensities of the various hyperfine-structure components of the 535 nm Tl line are shown in Figure 2. These wave numbers are based on hyperfine splittings and isotope shifts of thallium obtained by Odintsov [6]. Under our experimental conditions only two hyperfine-structure components are seen. A typical interferogram of the 535 nm line obtained in the present work for the spacer of 0.845 cm is shown in Figure 3. The hyperfine-structure components are resolved. Both the maxima correspond to the groups B_n, C_n, b_n, c_n, and A_n, and a_n, respectively, of hfs components in the interferogram of n-th order. Let us note that in Figs. 2 and 3 the origin of the wave number scale is shifted to the center of gravity of the 535 nm line.

In most cases we used the Fabry-Perot interferometer with the spacer of 1.204 cm. For this spacer the free spectral range of 0.415 cm^{-1} is approximately equal to the hyperfine-structure splitting of the 535 nm line. A typical interferogram is shown in Figure 4. It must be emphasized, however, that this interferogram does not correspond to the profile of an isolated line because the components C_n, B_n, c_n, b_n, and A_{n+1}, a_{n+1} of the interferograms of orders n, and $(n+1)$ respectively, overlap with one another. Since the separation between the hfs components C_n and A_{n+1}, c_n and a_{n+1} is small we can include in our numerical analysis of line profiles four components: $C_n + A_{n+1}$, B_n, $c_n + a_{n+1}$, b_n. In previous work done in this laboratory [2, 7] the numerical analysis was per-

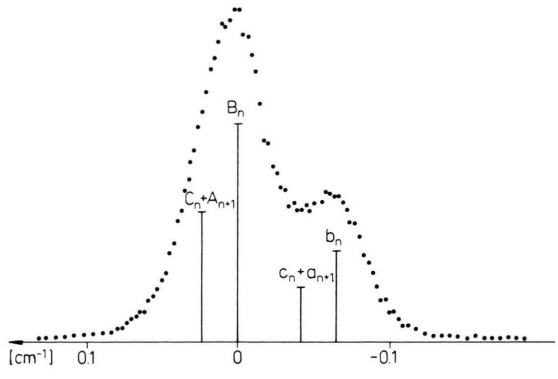

Fig. 4. Fabry-Perot interferogram of the 535 nm Tl line taken at the particle density $N = 2.4 \times 10^{17}\,\mathrm{cm}^{-3}$ of Ne with the spacer of 1.204 cm. Wave numbers (with respect to the component B_n) and relative intensities of four hfs components of this line are shown.

formed using a more simplified method in which only two components were taken into account.

In our analysis we have assumed that the pressure broadening and shift of all components of the line is the same. We have also assumed that the intensity distribution in a broadened line resulting from both Doppler and pressure broadening can be described by the Voigt profile, with the Lorentzian full half-width γ_L and shift Δ proportional to the number density of perturbers N, and with the density independent Gaussian half-width γ_D corresponding to the Doppler temperature of a gas. The measured line profile $I(\nu)$ is the convolution of the Voigt profile and the instrumental profile of the Fabry-Perot interferometer. Following Ballik [8] this convolution can be written in the form

$$I(\nu) = A \sum_{k=1}^{p} \eta_k \left\{ \frac{1}{2} + \sum_{m=1}^{\infty} (R\, e^{-L})^m \exp(-0.25\, D^2 m^2) \cdot \cos \frac{2\pi}{\Delta \nu_i} m (\nu - \nu_s - d_k - \Delta) \right\}, \quad (1)$$

where p is the number of line components, ν_s is the wave number of the strongest component, η_k denotes the relative intensity of the k-th component of a line and d_k is its shift relative to the strongest component. A is a normalizing factor independent of the wave number ν. In (1) R is the reflection coefficient of the etalon plates and $\Delta\nu_i$ denotes the free spectral range of the interferometer. The dimensionless parameters L and D are connected with the Lorentzian and Gaussian half-width γ_L and γ_G^* by the formulae

$$L = \frac{\pi}{\Delta \nu_i} \gamma_L \quad (2)$$

and

$$D = \frac{\pi}{\Delta \nu_i \sqrt{\ln 2}} \gamma_G^*. \quad (3)$$

The experimental values of the Lorentzian and Gaussian half-width γ_L and γ_G^* as well as the pressure shift Δ of the 535 nm Tl line reported in this work were determined by a least-squares fit of measured profiles to (1) using an algorithm given by Marquardt [9].

It should be noted that (1) was originally derived by Ballik [8] for an ideal Fabry-Perot interferometer for which the instrumental function is given by an Airy profile. Its width depends on the reflection coefficient R of the etalon plates only. In such a case γ_G^* can be identified with the Doppler half-width γ_D resulting from the thermal motion of emitting atoms with the Maxwellian distribution of velocities. It is given by [10]

$$\gamma_D = 2 \frac{\nu_0}{c} \sqrt{\frac{2 k_B}{M} \ln 2}, \quad (4)$$

where ν_0 is the unperturbed wave number of a line, M is the mass of the emitting atom, T is the temperature and k_B the Boltzmann constant.

We should emphasize, however, that in the case of a real Fabry-Perot interferometer the Airy-type profile appears to be a rather poor approximation to the instrumental function. This is caused by various imperfections of the interferometer, mainly those due to the deviation of the surfaces of the etalon plates from an ideal plane, as well as those due to slight inclinations of the two surfaces. These imperfections lead to the decrease of the total finesse of the real interferometer in comparison with its "ideal" value which is determined by the reflection coefficient of the etalon plates only. This effect gives rise to an additional instrumental broadening [11].

Its contribution to the instrumental profile of the real Fabry-Perot interferometer can be approximated by a Gaussian profile with the half-width $\gamma_G^{(a)}$. In such an approximation Ballik's formula (1) can also be used in the analysis of line profiles by means of real interferometers. In this case, however, γ_G^* plays

the role of an effective Gaussian half-width which is connected with $\gamma_G^{(a)}$ and the Doppler-half-width γ_D by the formula

$$\gamma_G^* = \sqrt{\gamma_D^2 + (\gamma_G^{(a)})^2}\,. \tag{5}$$

The half-widths $\gamma_G^{(a)}$ of the Gaussian component of the instrumental profile of the Fabry-Perot interferometer used in this work were estimated as $0.013\,\mathrm{cm}^{-1}$ and $0.020\,\mathrm{cm}^{-1}$ for the spacers of 1.204 cm and 0.845 cm respectively.

In the present work the numerical analysis of interferograms was performed by taking into account the full hyperfine structure of the 535 nm line emitted by natural thallium which consists of six components ($p = 6$ in (1)).

In previous experiments in this laboratory [2, 3, 7] a simplified analysis was carried out for two components ($p = 2$) only. We therefore made a test in order to establish how the parameters γ_L and γ_G^* depend on the number p of components used in the numerical analysis. The results of this test-analysis are listed in Table 1 for $p = 2$, 4 and 6. This analysis shows that the Gaussian half-widths γ_G^* obtained from the two-component approximation are significantly greater than those resulting from the four- or six-component analysis. It is interesting to note that the Lorentzian half-widths γ_L obtained in the two-component approximation are only slightly smaller than those resulting from the analysis in which the full hyperfine structure is taken into account.

Special attention in the present work was focused on the influence of reabsorption on the measured line profiles. We have found that under our experimental conditions the effects caused by reabsorption may be neglected.

Table 1. The Lorentzian γ_L and the effective Gaussian γ_G^* half-widths of the 535 nm Tl line perturbed by Ne and Ar determined for three values p of hfs components used in the numerical analysis (spacer of 1.204 cm).
Interferogram I: Neon density $4.9 \times 10^{17}\,\mathrm{cm}^{-3}$.
Interferogram II: Argon density $0.9 \times 10^{17}\,\mathrm{cm}^{-3}$.

The number p of hfs components	Interferogram I		Interferogram II	
	γ_L $10^{-3}\,\mathrm{cm}^{-1}$	γ_G^* $10^{-3}\,\mathrm{cm}^{-1}$	γ_L $10^{-3}\,\mathrm{cm}^{-1}$	γ_G^* $10^{-3}\,\mathrm{cm}^{-1}$
6	11.70	31.10	3.06	40.53
4	11.94	31.03	3.12	40.62
2	10.63	41.60	2.24	48.70

4. Results and Interpretation

As can be seen (see Fig. 5) γ_G^* is practically independent of the perturbing gas density. The average values of γ_G^* at a temperature of 793 K with the spacer of 1.204 cm were found to be $0.030\,\mathrm{cm}^{-1}$ for Tl + Ne and $0.042\,\mathrm{cm}^{-1}$ for Tl + Ar. The Doppler half-width γ_D calculated from (4) for 793 K is equal to $0.026\,\mathrm{cm}^{-1}$. In the case of Tl + Ne the discrepancy between γ_G^* and γ_D can also be explained on the grounds of (5) as a result of the contribution of the Gaussian component of the instrumental profile. For Tl + Ar, however, the average value of γ_G^* is slightly higher than that resulting from (5).

Figure 6 shows the Lorentzian half-width γ_L of the 535 nm Tl line plotted against the number density of perturbers. As can be seen, the Lorentzian half-width of this line depends linearly on the density in accordance with the impact theory of pressure broadening. The straight line in Fig. 6 is determined by least-squares fitting. The linear dependence of the Lorentzian half-width γ_L on the number density of perturbers N can be written as

$$\gamma_L = \gamma_0 + \beta N\,, \tag{6}$$

where β is the pressure broadening coefficient related to the interaction between the radiating Tl-atom and the perturbing atom. In (6) γ_0 is the sum of the natural width of the line and the residual Lorentzian half-width of the instrumental function.

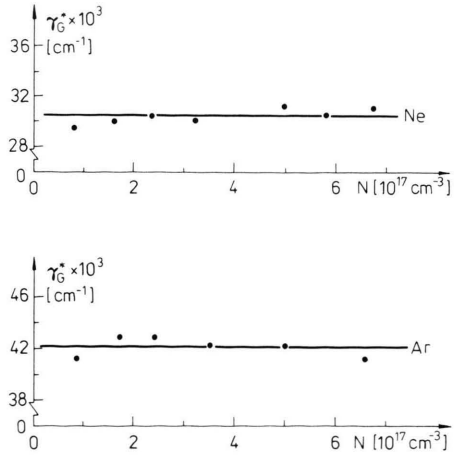

Fig. 5. The effective Gaussian full half-width γ_G^* of the 535 nm Tl line as a function of the particle density of the perturbing gas for the cases of Ne and Ar (spacer of Fabry-Perot interferometer 1.204 cm).

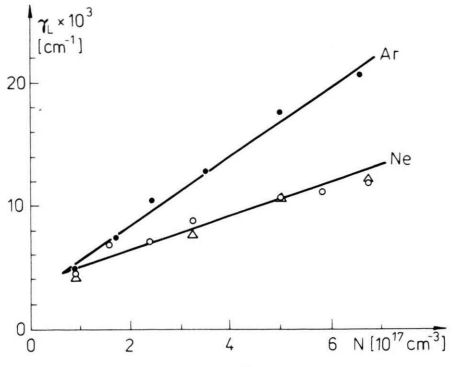

Fig. 6. The Lorentzian full half-width γ_L of the 535 nm Tl line as a function of the particle density of the perturbing gas:
● Ar for the spacer of 1.204 cm,
○ Ne for the spacer of 1.204 cm,
△ Ne for the spacer of 0.845 cm.

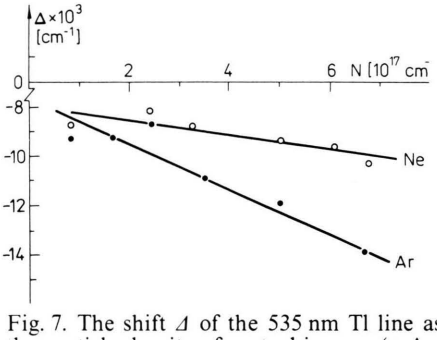

Fig. 7. The shift Δ of the 535 nm Tl line as a function of the particle density of perturbing gas (● Ar, ○ Ne) for the spacer of 1.204 cm.

Experimental values of β are listed in Table 2, where they are compared with the results determined by Cheron et al. [1] and by Lisicki et al. [2]. It must be remembered, however, that Cheron's experiment was carried out at perturbing gas densities two orders of magnitude higher ($(0.6-2.0) \times 10^{19}$ cm^{-3}) than those ($(0.1-7.0) \times 10^{17}$ cm^{-3}) used in the present investigation. On the other hand, the data of Lisicki et al. were obtained from experiments on the 535 nm thallium line resulting from the photodissociation of thallium iodide.

Figure 7 shows the plot of the shift Δ of the 535 nm Tl line against the number density of perturbers. For both neon and argon the shift is linear over the density range measured according to the relation

$$\Delta = \Delta_0 + \delta N, \tag{7}$$

where δ denotes the pressure shift coefficient corresponding to the interaction of the radiating Tl atom with the perturbing atom. In (7) the quantity Δ_0 comprises the shift of the line in the reference source and that resulting from the numerical data analysis. As can be seen in Fig. 7 neon and argon produce a red shift (minus sign) of the 535 nm Tl line.

The values δ of the pressure shift coefficient determined from the slopes of the straight lines shown in Fig. 7 are listed in Table 3, where they are

Table 2. Experimental and theoretical values of the pressure broadening coefficient β (in units 10^{-20} cm^{-1}/atom cm^{-3}). Numbers in parentheses are standard deviations of the least-squares fit.

Perturber	Experiment			Theory					
	This work	Cheron et al. [1]	Lisicki et al. [2]	Lennard-Jones			Van der Waals		
				coul	H-F	D-H-F	coul	H-F	D-H-F
Ne	1.11 (0.12)	1.49 (0.15)	1.45 (0.03)	1.52	2.07	1.72	1.75	1.98	1.82
Ar	2.74 (0.18)	3.12 (0.22)	3.36 (0.09)	2.00	1.99	1.84	2.58	2.90	2.67

Table 3. Experimental and theoretical values of the pressure shift coefficient Δ (in units 10^{-20} cm^{-1}/atom cm^{-3}). Numbers in parentheses are standard deviations of the least-squares-fit.

Perturber	Experiment			Theory					
	This work	Cheron et al. [1]	Lisicki et al. [2]	Lennard-Jones			Van der Waals		
				coul	H-F	D-H-F	coul	H-F	D-H-F
Ne	− 0.24 (0.10)	− 0.32 (0.07)	− 0.34 (0.02)	− 0.14	− 0.07	− 0.08	− 0.64	− 0.72	− 0.68
Ar	− 0.87 (0.12)	− 1.00 (0.07)	− 0.98 (0.01)	− 1.10	− 1.04	− 0.99	− 0.94	− 1.06	− 0.97

compared with the experimental values obtained by Cheron et al. [1] and Lisicki et al. [2].

The theoretical values of β and Δ for the 535 nm Tl line were calculated in our previous paper [2] for the Lennard-Jones and Van der Waals potentials. The constants C_6 and C_{12} of the Lennard-Jones function have been calculated using three methods. The first method (coul) consists of the application of a simple Coulomb approximation introduced by Unsöld [10]. In the remaining two methods either non-relativistic Hartree-Fock (H-F) wave functions or multiconfiguration relativistic Dirac-Hartree-Fock (D-H-F) wave functions have been applied. The values of β and δ obtained from the Lindholm-Foley impact theory for these values of C_6 and C_{12} are listed in Tables 2 and 3. It should be noted that our measured values of β and Δ for Tl + Ar are in reasonable agreement with theoretical values of Wu et al. [12] (calculated for the Van der Waals potentials using the C_6 constant computed by Proctor and Stwalley [13]), as well as with those computed by Czuchaj et al. [14].

5. Conclusion

The comparison of experimental results determined in the present work (Tables 2 and 3) with those obtained in earlier investigations shows that our values of β and δ are smaller than both the width and shift parameters obtained by Cheron et al. [1] in their high-pressure emission study, and the values by Lisicki et al. [2] from the photodissociation experiment performed on thallium iodide vapour. However, the discrepancies between these three sets of experimental data obtained by means of different experimental techniques are not large. Special attention in the present study was focused on the problem of accuracy in determining the width of the Gaussian component of the profile. We have found that in the case of the spectral line with a complex hyperfine structure a very careful numerical analysis of the Fabry-Perot interferograms is necessary to obtain reliable results for the Gaussian width. In particular it turned out that the Gaussian width is much more sensitive to the finesse of the Fabry-Perot etalon than the width of the Lorentzian component of the total profile. The results of the present work corroborate the conclusion given in [2] that for Tl + Ar and Tl + Ne the purely attractive Van der Waals potentials lead to reasonable agreement of the theoretical values of β and δ for the 535 nm line with the measured ones.

Acknowledgements

The authors are grateful to the referee for several helpful criticisms of the original manuscript.

[1] B. Cheron, R. Scheps, and A. Gallagher, J. Phys. **A 15,** 651 (1977).
[2] E. Lisicki, A. Bielski, and J. Szudy, Z. Naturforsch. **35 a,** 1249 (1980); **36 a,** 807 (1981).
[3] E. Lisicki, A. Bielski, J. Szudy, and J. Wolnikowski, Z. Naturforsch. **40 a,** 800 (1985).
[4] R. N. Zare and D. R. Herschbach, Proc. IEEE **51,** 173 (1963).
[5] A. Bielski, S. A. Kandela, J. Wolnikowski, and Z. Turło, Acta Phys. Polon. **A 42,** 295 (1972); A. Bielski, W. Dokurno, E. Lisicki, and Z. Turlo, Optica Applicata **11,** 151 (1981).
[6] A. J. Odintsov, Optics and Spectrosc. **9,** 75 (1960).
[7] E. Lisicki, A. Bielski, and J. Szudy, Acta Phys. Polon. **A 56,** 557 (1979).
[8] E. A. Ballik, Appl. Opt. **5,** 170 (1966).
[9] D. W. Marquardt, J. Soc. Indust. Appl. Math. **11,** 431 (1963).
[10] A. Unsöld, Physik der Sternatmosphären. Springer-Verlag, Berlin 1955.
[11] W. Dömtreder, Laser Spectroscopy. Springer-Verlag, Berlin 1981, p. 152–160.
[12] C. Y. Wu, W. C. Stwalley, and T. R. Proctor, J. Chem. Phys. **61,** 4328 (1978).
[13] T. R. Proctor and W. C. Stwalley, J. Chem. Phys. **66,** 2063 (1977).
[14] E. Czuchaj and J. Sienkiewicz, Z. Naturforsch. **39 a,** 513 (1984).